European Congress on Computational Methods
in Applied Sciences and Engineering (ECCOMAS 2012)
J. Eberhardsteiner et.al. (eds.)
Vienna, Austria, September 10-14, 2012

USING A LEVEL SET TO MODEL MULTIPLE MYELOMA INDUCED BONE LOSS

Bruce P. Ayati[1], **Jason M. Graham**[2], **and Sarah A. Holstein**[3]

[1]Department of Mathematics and Program in Applied Mathematical and Computational Sciences
University of Iowa
Iowa City, IA 52242-1419 USA
e-mail: bruce-ayati@uiowa.edu

[2]Department of Mathematics and Program in Applied Mathematical and Computational Sciences
University of Iowa
Iowa City, IA 52242-1419 USA
e-mail: jason-graham@uiowa.edu

[3]Department of Internal Medicine
University of Iowa
Iowa City, IA 52242-1081 USA
e-mail: sarah-holstein@uiowa.edu

Keywords: multiple myeloma, bone remodeling, level set

Abstract. *Multiple myeloma is a hematological malignancy characterized by proliferation of malignant plasma cells and derangement of bone homeostasis. Myeloma bone disease results in significant morbidity as a result of bone pain, hypercalcemia, diffuse osteopenia, and pathologic fractures.*

We present a spatially explicit mathematical model of multiple myeloma and bone remodeling, synthesizing the existing model of local "microenvironment" interactions in Ayati et al. 2010 [1] with a level set approach for representing the sharp interface been bone and marrow introduced in [6]. Computational results show the feasibility of using a level set to capture the spatial structure in the context of a geometrically straightforward interface, but one that nonetheless captures the essence of the rich geometries seen in bone marrow biopsy slides. In particular, we are able to model the formation of an osteolytic lesion in the case of multiple myeloma dysregulated bone remodeling, but not, using the same remodeling parameter set, in the case of normal bone remodeling.

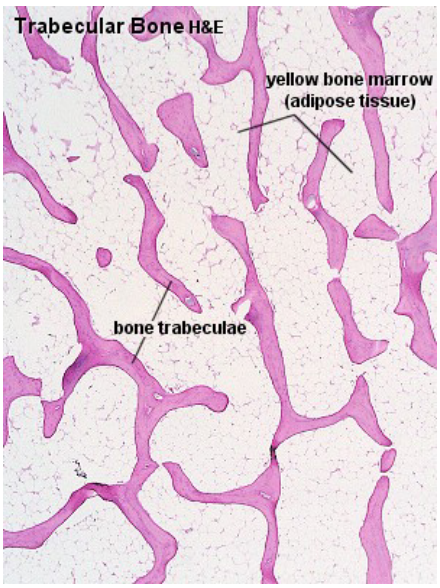

Figure 1: A slice of trabecular bone showing the sharp, rather than diffuse, interface between bone and marrow when viewed at scales larger than that of a single bone multicellular unit (BMU). Note the rich geometry of the interface. Figure courtesy of Lutz Slomianka of the School of Anatomy and Human Biology at The University of Western Australia.

1 Introduction

Bone disease is a major contributor to the morbidity and mortality of multiple myeloma. Osteolytic bone lesions cause hypercalcemia, bone pain, and pathologic fractures. Vertebral involvement can lead to spinal cord compression and severe neurological compromise. It is estimated that 60% of all myeloma patients will present with bone pain at the time of diagnosis. In addition, nearly 80% of patients will have osteolytic lesions, diffuse osteopenia, or fractures found in skeletal surveys at the time of diagnosis [11]. Furthermore, in one study, 50% of patients with a negative skeletal survey were found to have lesions on MRI [28]. Almost 50% of patients will have a pathologic fracture during the course of their disease and this is associated with an increased risk of death compared to those patients without fractures [25].

A range of mathematical models of the bone remodeling process exist in the literature [2, 3, 4, 6, 10, 8, 9, 12, 14, 15, 17, 18, 19, 20, 21, 22, 26]. Less has been done on the interaction between multiple myeloma and the bone remodeling process. The relatively recent manuscript by Ayati, Edwards, Webb and Wikswo in 2010 [1] is to our knowledge the first work to investigate the so-called multiple myeloma and bone "vicious cycle." The model in this first effort is phenomenological rather than mechanistic, and the diffusion terms used to represent the spatial dynamics are accurate only for very small spatial scales and short time scales. Alternate approaches also exist. For example, there is increasing understanding of the biochemical basis for the interactions between myeloma cells, osteoclasts, and osteoblasts in the vicious cycle. Wang, Pivonka, Buenzli, Smith and Dunstan in 2011 [29] incorporated much of this work into a mathematical model. For simplicity and better correlation between model elements and what is observed in bone marrow biopsies, we retain the approach of [1]. Moreover, the model in [1] has well understood mathematical properties and has been included in the BioModels Database (http://www.ebi.ac.uk/biomodels-main/)[1].

[1] At http://www.ebi.ac.uk/biomodels-main/BIOMD0000000401 for normal bone remodeling (essentially the model in [10]) and http://www.ebi.ac.uk/biomodels-main/BIOMD0000000402 with multiple myeloma.

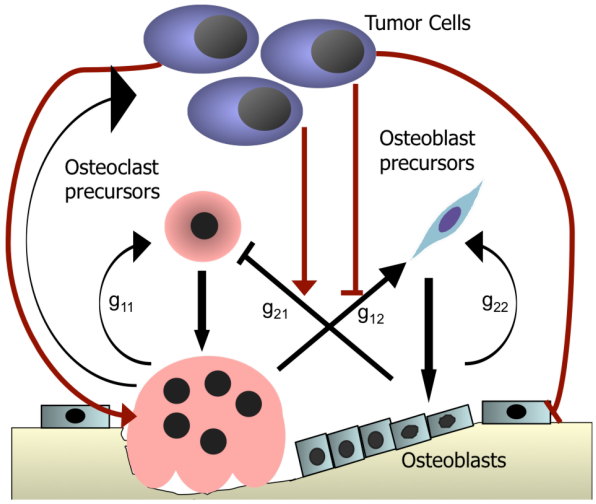

Figure 2: Schematic from [1] showing the multiple myeloma and bone vicious cycle with corresponding power law coefficients. This model ignores the role of osteocytes and stromal cells in the multiple myeloma and bone "vicious cycle." We retain this simpler model of local "microenvironment" interactions for our spatial modeling in this paper.

Our modeling of the cellular level interactions in multiple myeloma and bone remodeling builds on the mathematical "power-law" formalism of Biochemical Systems Theory (BST) [13, 23, 27], used by initially by Komarova et al. in 2003 [10] for cellular interactions in bone remodeling. The model in [10] formed the basis of the multiple myeloma model in [1] that we use for the local cellular interactions in this paper.

Recent spatially explicit models of the bone remodeling process used diffusion and/or chemotaxis terms to model the movement of a tunneling bone multicellular unit (BMU) [2, 21, 22]. Our interest is on the larger spatial scales of bone marrow biopsies. We use a mathematical representation better suited for this spatial scale based on the level set method, an approach outlined in [6]. The interest in spatial structure on this scale is to build tools to investigate the degree that the bone and bone marrow morphology contains information about myeloma dysregulated bone disease not contained in cell counts and chemical densities alone. The geometries in trabecular bone are particularly rich (see Figure 1).

Computational results show the feasibility of using a level set to capture the spatial structure in the context of a geometrically straightforward interface, but one that nonetheless captures the essence of the rich geometries seen in bone marrow biopsy slides. In particular, we are able to model the formation of an osteolytic lesion in the case of multiple myeloma dysregulated bone remodeling, but not, for the same remodeling parameter set, in the case of normal bone remodeling.

2 Model of Local Interactions

The model of local "microenvironment" interactions is taken from [1] and based on the interactions shown in Figure 2. Essentially, bone remodeling involves the removal (also called "resorption") of bone by multinuclear osteoclasts and the rebuilding of new bone by osteoblasts. The recruitment of these cell types to a location is interdependent. In multiple myeloma dysregulated bone remodeling, the normal interplay between osteoclasts and osteoblasts is modified

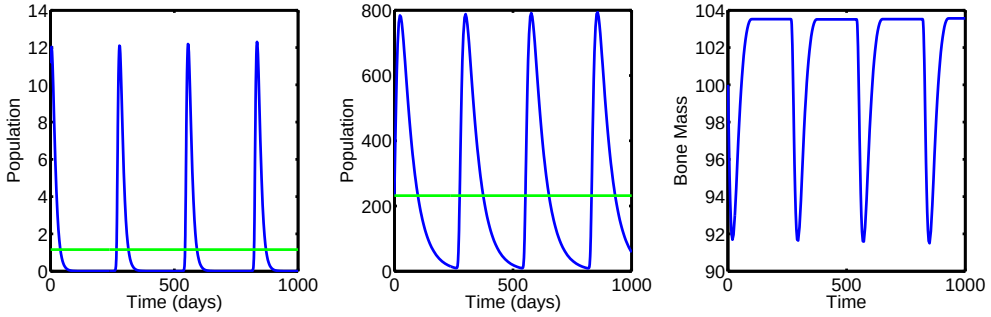

(a) Osteoclasts (b) Osteoblasts (c) Local Bone Mass

Figure 3: Komarova et al. 2003 model [10] dynamics for remodeling cells under normal bone remodeling ($r_{11} = r_{12} = r_{21} = r_{22} = 0$). The threshold values $\bar{C}$ and $\bar{B}$ are shown in green. We have regular periodicity in the system dynamics.

by tumor cells, resulting in net bone loss over time. We note that this model of the local interactions is highly simplified and is used for convenience and the established understanding of its mathematical properties [1]. This local model does not include complicating mechanisms that may make for a more faithful representation of the myeloma and bone vicious cycle, such as the inclusion of terms for osteocytes and stromal cells [5, 7, 30].

We summarize the local model below. The local system depends on time only. The dependent variables are

- $C(t) =$ osteoclast population density at time t.
- $B(t) =$ osteoblast population density at time t.
- $T(t) =$ tumor cell population density at time t.
- $z(t) =$ bone density at the remodeling site. This will be reinterpreted as bone thickness in the spatial model in Section 3.

For the model equations we use a power-law approach with the exponents modified by the tumor cells. We use a Gompertz law for tumor growth. Bone density is a function of bone remodeling activity. The local model is

$$\frac{dC}{dt} = \alpha_1 C^{g_{11}\left(1+r_{11}\frac{T}{L_T}\right)} B^{g_{21}\left(1+r_{21}\frac{T}{L_T}\right)} - \beta_1 C, \tag{1a}$$

$$\frac{dB}{dt} = \alpha_2 C^{\frac{g_{12}}{1+r_{12}\frac{T}{L_T}}} B^{\left(g_{22}-r_{22}\frac{T}{L_T}\right)} - \beta_2 B, \tag{1b}$$

$$\frac{dT}{dt} = \gamma_T T \log\left(\frac{L_T}{T}\right), \tag{1c}$$

$$\frac{dz}{dt} = -\kappa_1 \max\{0, C - \bar{C}\} + \kappa_2 \max\{0, B - \bar{B}\}, \tag{1d}$$

where we use steady-state values of osteoclast and osteoblast densities as thresholds for remod-

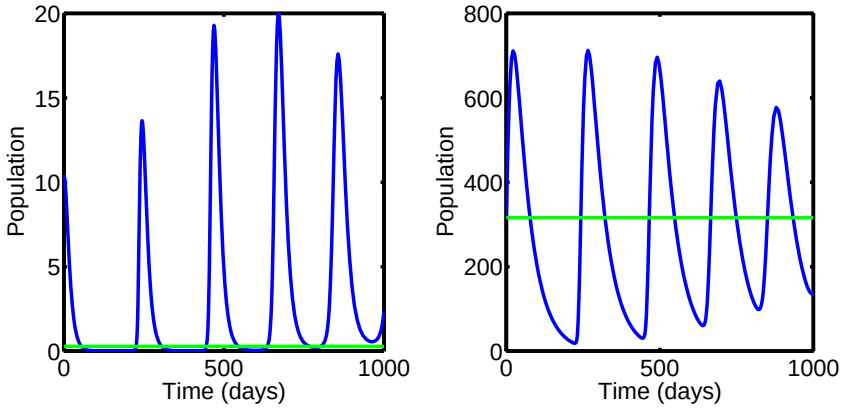

(a) Osteoclasts

(b) Osteoblasts

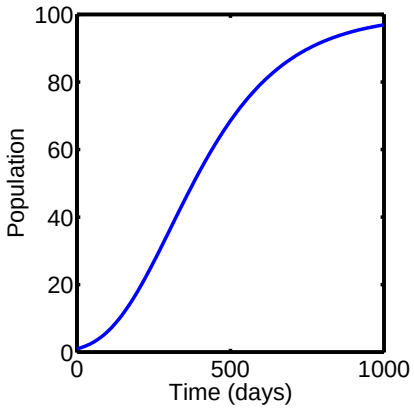

(c) Tumor Cells

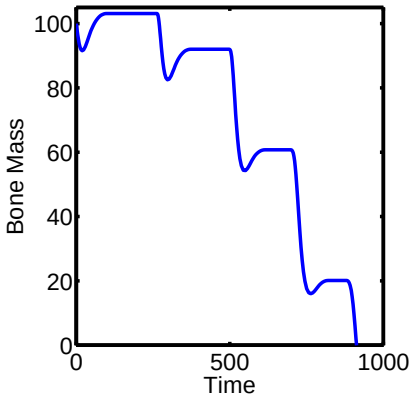

(d) Local Bone Mass

Figure 4: Ayati et al. model 2010 [1] dynamics for remodeling cells in the presence of multiple myeloma tumor cells ($r_{11} = 0.005$, $r_{12} = 0.0$, $r_{21} = 0.0$, $r_{22} = 0.2$), assuming only dysregulation of the autocrine signaling. The threshold values $\bar{C}$ and $\bar{B}$ are shown in green. We have an initial increase in osteoclasts and decrease in osteoblasts before the damping of the overall system due to takeover by multiple myeloma cells.

eling activity in (1d),

$$\bar{C} = \left(\frac{\alpha_1}{\beta_1}\right)^{\left(\frac{1-g_{22}-r_{22}}{\Lambda}\right)} \left(\frac{\alpha_2}{\beta_2}\right)^{\left(\frac{g_{21}}{\Lambda}\right)(1+r_{21})}, \tag{2a}$$

$$\bar{B} = \left(\frac{\alpha_1}{\beta_1}\right)^{\frac{\left(\frac{g_{12}}{1+r_{12}}\right)}{\Lambda}} \left(\frac{\alpha_2}{\beta_2}\right)^{\frac{1-g_{11}(1+r_{11})}{\Lambda}}, \tag{2b}$$

$$\Lambda = (1 - g_{11}(1 + r_{11}))(1 - g_{22} + r_{22}) - \left(\frac{g_{12}}{1 + r_{12}}\right)(g_{21}(1 + r_{21})). \tag{2c}$$

The use of these threshold values for remodeling activity accounts for the presence of precursor cell types in the osteoblast and osteoclast densities. A more complicated model would contain different compartments for precursor cell types.

The base parameter meanings are

- $\alpha_1 =$ coefficient of osteoclast recruitment.
- $\beta_1 =$ coefficient of osteoclast removal.

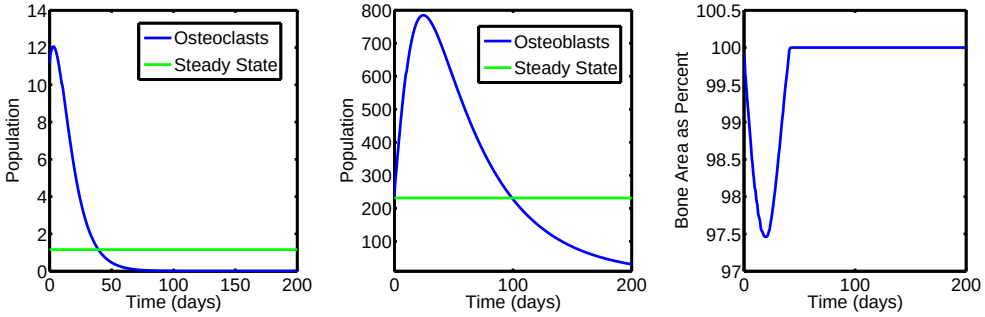

(a) Osteoclasts (b) Osteoblasts (c) Bone Area

Figure 5: Aggregation across space of the dynamics under normal bone remodeling ($r_{11} = r_{12} = r_{21} = r_{22} = 0$) of the spatially explicit model. Compare to one cycle in Figure 3, particularly Figure 5(c) to once cycle in Figure 3(c).

- $\alpha_1 =$ coefficient of osteoclast recruitment.
- $\beta_1 =$ coefficient of osteoclast removal.
- $g_{11} =$ strength of osteoclast self promotion ("autocrine" signaling).
- $g_{21} =$ strength of osteoblast promotion of osteoclasts ("paracrine" signaling).
- $g_{12} =$ strength of osteoclast promotion of osteoblasts ("paracrine" signaling).
- $g_{22} =$ strength of osteoblast self promotion ("autocrine" signaling).
- $L_T =$ tumor scaling density.
- $\gamma_T =$ Gompertz law coefficient.
- $\kappa_1 =$ bone loss coefficient due to osteoclast resorption.
- $\kappa_2 =$ bone gain coefficient due to osteoblast activity.

The parameters of interest are those for the role of the tumor:

- $r_{11} =$ tumor modification of osteoclast self promotion.
- $r_{21} =$ tumor modification of osteoblast promotion of osteoclasts.
- $r_{12} =$ tumor modification of osteoclast promotion of osteoblasts.
- $r_{22} =$ tumor modification of osteoblast self promotion.

The base parameters used in the computations are $\alpha_1 = 3$, $\beta_1 = 0.2$, $\alpha_2 = 4$, $\beta_2 = 0.02$, $g_{11} = 0.5$, $g_{21} = -0.5$, $g_{12} = 1$, $g_{22} = 0$, $L_T = 100$, $\gamma_T = 0.005$, $\kappa_1 = 0.0748$, and $\kappa_2 = 0.0006395$.

We show results for the local dynamics in the no tumor case ($r_{11} = r_{12} = r_{21} = r_{22} = 0$) in Figure 3. We have regular periodicity of all model components in the case of no tumor. We show the results for multiple myeloma dysregulated autocrine signaling in bone remodeling ($r_{11} = 0.005$, $r_{12} = 0.0$, $r_{21} = 0.0$, $r_{22} = 0.2$) in Figure 4. The dynamics show an initial oscillatory increase in osteoclasts and decrease in osteoblasts. As the tumor cell density increases, the entire bone remodeling system becomes damped and we get an oscillatory decrease in both osteoclast and osteoblast numbers, as well as bone mass.

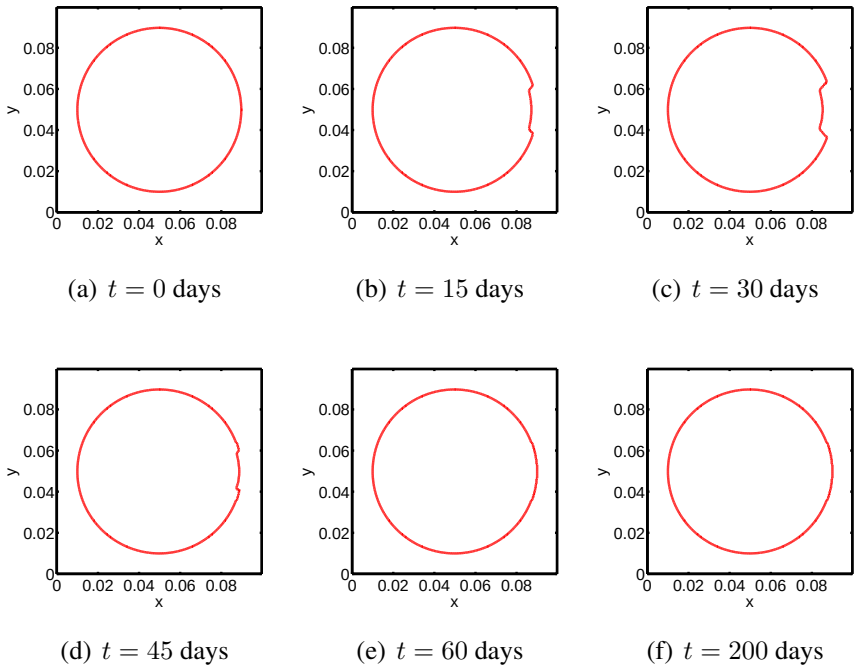

(a) $t = 0$ days (b) $t = 15$ days (c) $t = 30$ days

(d) $t = 45$ days (e) $t = 60$ days (f) $t = 200$ days

Figure 6: Bone and bone marrow interface snapshots in time in the case of normal bone remodeling. The interior of the circle is trabecular bone. The section of remodeled bone is fully reformed over time and absent of any development of an osteolytic lesion.

3 Dynamic Interface Model of Spatial Interactions

In this section we extend the spatially local models presented above from [1, 10] to a larger spatial domain using a level set representation, as was done for normal bone remodeling in [6]. We examine a slice of bone, so restrict our model to two spatial dimensions. We assume a sharp interface between trabecular bone and bone marrow and denote this interface by $\Gamma_t \subset \mathbb{R}^2$. The velocity of the interface is determined solely by local bone remodeling. Unlike many other applications of the level set method, curvature and other aspects of the local geometry play no role in the movement of the interface.

We relate Γ_t to a level set function $\phi(x,t)$ by the relationship $\Gamma_t = \{x = (x_1, x_2) \in \mathbb{R}^2 : \phi(x,t) = 0\}$. As summarized in [6] and discussed in much more detail in Osher and Fedkiw [16] and Sethian [24], the purpose of a level set is to represent an interface implicitly as the zero level set of a higher dimensional function. For example, we can describe a circle of radius 1 centered at $(0,0)$ explicitly using one independent variable as $(\cos t, \sin t)$ for $0 \leq t < 2\pi$, or implicitly using two independent variables by setting $\phi(x_1, x_2) = 1 - x_1^2 - x_2^2$. At first glance it might seem odd to add an extra complicating dimension to our problem, but as discussed in [16, 24], there are important advantages in moving an interface defined implicitly using a level set function over moving an interface defined by an explicit representation. Moreover, for our modeling needs, the level set provides a natural extension of the local model by allowing us to simply replace the term for change of bone mass with the velocity of the interface, using appropriate scaling constants.

Our system now depends on time and space with dependent variables

- $C(x,t) =$ osteoclast population density at position $x \in \mathbb{R}^2$ and time t,
- $B(x,t) =$ osteoblast population density at position $x \in \mathbb{R}^2$ and time t,

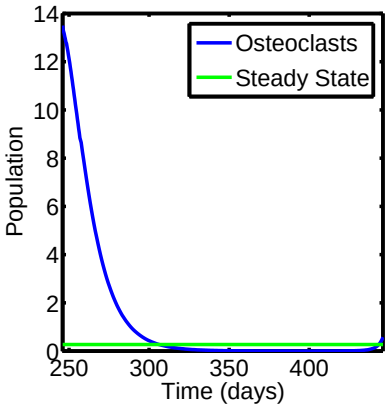

(a) Osteoclasts

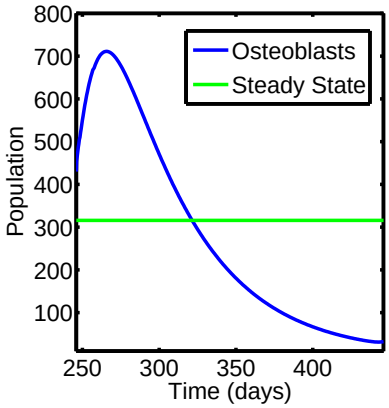

(b) Osteoblasts

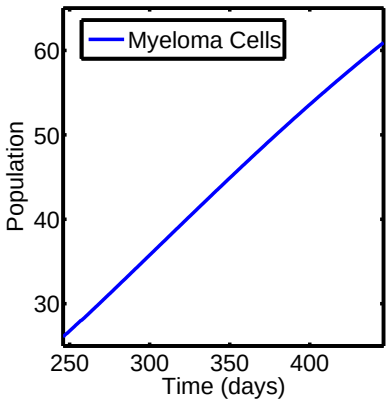

(c) Tumor Cells

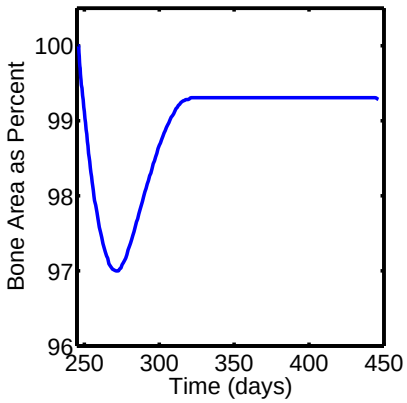

(d) Bone Area

Figure 7: Aggregation across space of the dynamics under multiple myeloma dysregulated bone remodeling ($r_{11} = 0.005$, $r_{12} = 0.0$, $r_{21} = 0.0$, $r_{22} = 0.2$) of the spatially explicit model. Compare to one cycle in Figure 4, particularly Figure 7(d) to one cycle in Figure 4(d). In this model we see a net loss of bone in the course of one remodeling cycle.

- $T(x,t) =$ tumor cell population density at position $x \in \mathbb{R}^2$ and time t,
- $a(x,t) =$ velocity of the bone and marrow interface at position $x \in \Gamma_t \subset \mathbb{R}^2$ and time t.

The local model is extended to the spatial system

$$\frac{dC}{dt} = \alpha_1 C^{g_{11}\left(1+r_{11}\frac{T}{L_T}\right)} B^{g_{21}\left(1+r_{21}\frac{T}{L_T}\right)} - \beta_1 C, \tag{3a}$$

$$\frac{dB}{dt} = \alpha_2 C^{\frac{g_{12}}{1+r_{12}\frac{T}{L_T}}} B^{\left(g_{22}-r_{22}\frac{T}{L_T}\right)} - \beta_2 B, \tag{3b}$$

$$\frac{dT}{dt} = \gamma_T T \log\left(\frac{L_T}{T}\right), \tag{3c}$$

$$\frac{d\phi}{dt} + a\|\nabla\phi\| = 0, \tag{3d}$$

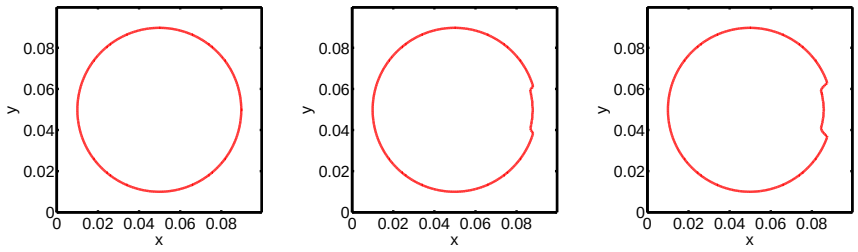

(a) $t = 246$ days (b) $t = 261$ days (c) $t = 276$ days

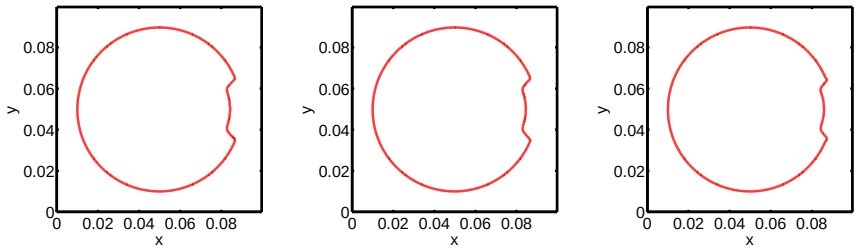

(d) $t = 291$ days (e) $t = 306$ days (f) $t = 321$ days

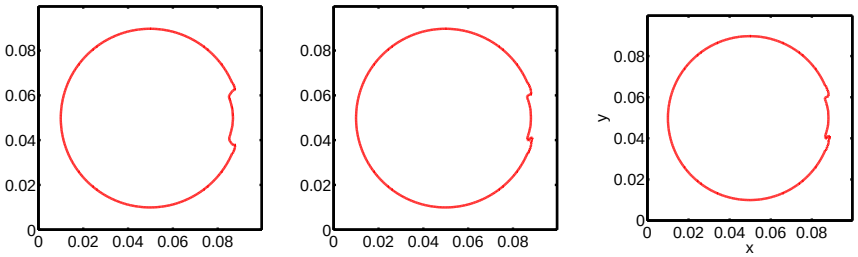

(g) $t = 336$ days (h) $t = 351$ days (i) $t = 446$ days

Figure 8: Bone and bone marrow interface snapshots in time in the case of multiple myeloma dysregulated bone remodeling. The interior of the circle is trabecular bone. The section of remodeled bone is not fully restored and we see the beginning of the development of an osteolytic lesion.

with

$$a(x,t) = -k_1 \max\{0, C - \bar{C}\} + k_2 \max\{0, B - \bar{B}\}, \tag{3e}$$

$$C(x,t) = \tilde{C}(x,t),\ x \in \Gamma_t, \tag{3f}$$

$$B(x,t) = \tilde{B}(x,t),\ x \in \Gamma_t, \tag{3g}$$

$$T(x,t) = \tilde{T}(x,t),\ x \in \Gamma_t, \tag{3h}$$

$$\phi(x,0) = \phi_0(x), \tag{3i}$$

where the rate of change of bone mass $\frac{dz(t)}{dt}$ in the local model has been replaced by a velocity term for the bone and bone marrow interface, $a(x,t)$. We use new, dimensionally relevant scaling constants k_1 and k_2 instead of κ_1 and κ_2.

The computational results for the level set model of normal bone remodeling are shown in Figures 5 and 6 for one remodeling cycle. Parameters are the same as the local model, with the replacement of scaling constants with $k_1 = 0.001\kappa_1 = 0.0000748$ and $k_2 = 0.001\kappa_2 = 0.0000006395$. Figure 5 shows aggregate results across space and matches what we see in the

computational results for the spatially local model of normal bone remodeling. Namely, a return of bone mass after remodeling to the original amount. Spatially, in Figure 6 we begin with an idealized circular geometry for the bone and bone marrow interface (the interior of the circle is trabecular bone). After an area of bone is resorbed and reformed, the bone and bone marrow interface returns to its original shape, absent of anything that would indicate an osteolytic lesion.

The computational results for the level set model of normal bone remodeling are shown in Figures 7 and 8 for one remodeling cycle. Again, Figure 7 shows aggregate results across space and matches what we see in the computational results for the spatially local model of myeloma dysregulated bone remodeling. We also again begin with an idealized circular geometry in Figure 8, but now the effects of multiple myeloma manifest themselves as a net loss of bone mass at the remodeling site over a remodeling cycle, in essence the beginning of the formation of an osteolytic lesion. Like in the normal remodeling case, using an idealized geometry for these initial computations helps us visualize the formation of an osteolytic lesion more clearly than using a more complicated geometry.

4 Conclusions

In this paper we have shown the feasibility of using a level set to capture the geometries in bone marrow biopsy slides. We used a simplified model of the local "microenvironment" interactions that nonetheless captures the bone remodeling cycle, and embedded it into a level set model for the spatial interactions. It is a matter of bookkeeping, rather than additional genuine mathematical complexity, to replace our idealized circular geometry with the richer actual geometries seen in bone marrow biopsies such as Figure 1. The use of an idealized circular geometry also allows us to see clearly the formation of an osteolytic lesion in the computations with tumor load (Figure 8), and the absence of such lesions in the case of normal bone remodeling (Figure 6).

The ability to model faithfully the skeletal effects of multiple myeloma will provide insight into the pathological relationship between multiple myeloma cells and the sounding bone marrow environment, and improved understanding of this disease's morbidity [11, 25, 28].

Acknowledgments

We thank Lutz Slomianka for use of the photograph in Figure 1. BA was partially supported by NSF grant DMS-0914514. SH was partially supported by the PhRMA Foundation Faculty Development Award and the Carver Charitable Trust Young Investigator Award.

REFERENCES

[1] Bruce P. Ayati, Claire M. Edwards, Glenn F. Webb, and John P. Wikswo. A mathematical model of bone remodeling dynamics for normal bone cell populations and myeloma bone disease. *Biology Direct*, 5(28):1–15, May 2010.

[2] P R Buenzli, P Pivonka, and D W Smith. Spatio-temporal structure of cell distribution in cortical bone multicellular units: a mathematical model. *Bone*, 48(4):918–26, April 2011.

[3] J M García-Aznar, T Rueberg, and M Doblare. A bone remodelling model coupling microdamage growth and repair by 3D BMU-activity. *Biomech Model Mechanobiol*, 4(2-3):147–167, November 2005.

[4] Liesbet Geris, Alf Gerisch, and Richard C Schugart. Mathematical Modeling in Wound Healing, Bone Regeneration and Tissue Engineering. *Acta Biotheor*, pages 1–13, July 2010.

[5] N Giuliani, M Ferretti, M Bolzoni, P Storti, M Lazzaretti, B Dalla Palma, S Bonomini, E Martella, L Agnelli, a Neri, F Ceccarelli, and C Palumbo. Increased osteocyte death in multiple myeloma patients: role in myeloma-induced osteoclast formation. *Leukemia : official journal of the Leukemia Society of America, Leukemia Research Fund, U.K*, (November 2011):1–11, January 2012.

[6] Jason M. Graham, Bruce P. Ayati, Prem S. Ramakrishnan, and James A. Martin. Towards a New Spatial Representation of Bone Remodeling. *Mathematical Biosciences and Engineering*, 9(2):281–295, 2012.

[7] David Killock. Osteocyte RANKL in bone homeostasis: a paradigm shift? *Nature Reviews Rheumatology*, 7(11):619, November 2011.

[8] S V Komarova. Mathematical Model of Paracrine Interactions between Osteoclasts and Osteoblasts Predicts Anabolic Action of Parathyroid Hormone on Bone. *Endocrinology*, 146(8):3589–3595, April 2005.

[9] S V Komarova. Bone Remodeling in Health and Disease: Lessons From Mathematical Modeling. *Annals of the New York Academy of Sciences*, 1068(1):557–559, April 2006.

[10] Svetlana V. Komarova, Robert J. Smith, S. Jeffrey Dixon, Stephen M. Sims, and Lindi M. Wahl. Mathematical model predicts a critical role for osteoclast autocrine regulation in the control of bone remodeling. *Bone*, 33:206–215, January 2003.

[11] Robert A. Kyle, Morie A. Gertz, Thomas E. Witzig, John A. Lust, Martha Q. Lacy, Angela Dispenzieri, Rafael Fonseca, S. Vincent Rajkumar, Janice R. Offord, Dirk R. Larson, Matthew E. Plevak, Terry M. Therneau, and Philip R. Greipp. Review of 1027 Patients with Newly Diagnosed Multiple Myeloma. *Mayo Clin Proc*, 78(1):21–33, January 2003.

[12] Vincent Lemaire, Frank L Tobin, Larry D Greller, Carolyn R Cho, and Larry J Suva. Modeling the interactions between osteoblast and osteoclast activities in bone remodeling. *Journal of theoretical biology*, 229(3):293–309, August 2004.

[13] Anna Machina, Arkady Ponosov, and Eberhard O Voit. Automated piecewise power-law modeling of biological systems. *Journal of Biotechnology*, 149(3):154–65, September 2010.

[14] A Moroz, M C Crane, G Smith, and D I Wimpenny. Phenomenological model of bone remodeling cycle containing osteocyte regulation loop. *Biosystems*, 84(3):183–190, 2006.

[15] A Moroz and D I Wimpenny. Allosteric control model of bone remodelling containing periodical modes. *Biophysical Chemistry*, 127(3):194–212, 2007.

[16] Stanley J. Osher and Ronald P. Fedkiw. *Level Set Methods and Dynamic Implicit Surfaces*. Springer, 2003.

[17] Peter Pivonka and Svetlana V Komarova. Mathematical modeling in bone biology: From intracellular signaling to tissue mechanics. *Bone*, 47(2):181–189, July 2010.

[18] Peter Pivonka, Jan Zimak, David W Smith, Bruce S Gardiner, Colin R Dunstan, Natalie A Sims, T John Martin, and Gregory R Mundy. Model structure and control of bone remodeling: A theoretical study. *Bone*, 43:249–263, January 2008.

[19] J M Restrepo, R Choksi, J M Hyman, and Y Jiang. Improving the damage accumulation in a biomechanical bone remodelling model. *Computer Methods in Biomechanics and Biomedical Engineering*, 12(3):341–352, January 2009.

[20] Romain Rieger, Ridha Hambli, and Rachid Jennane. Modeling of biological doses and mechanical effects on bone transduction. *Journal of Theoretical Biology*, 274(1):36–42, 2011.

[21] Marc D Ryser, Svetlana V Komarova, and Nilima Nigam. The Cellular Dynamics of Bone Remodeling: A Mathematical Model. *SIAM J. Appl. Math.*, 70(6):1899–1921, February 2010.

[22] Marc D Ryser, Nilima Nigam, and Svetlana V Komarova. Mathematical Modeling of Spatio-Temporal Dynamics of a Single Bone Multicellular Unit. *Journal of Bone and Mineral Research*, 24(5):860–870, May 2009.

[23] Michael A. Savageau, Eberhard O. Voit, and Douglas H. Irvine. Biochemical Systems Theory and Metabolic Control Theory : 1 . Fundamental Similarities and Differences. *Mathematical Biosciences*, 86:127–145, 1987.

[24] J. A. Sethian. *Level Set Methods and Fast Marching Methods*. Cambridge University Press, 1999.

[25] Mehmet Sonmez, Tulin Akagun, Murat Topbas, Umit Cobanoglu, Bircan Sonmez, Mustafa Yilmaz, Ercument Ovali, and Serdar Bedii Omay. Effect of pathologic fractures on survival in multiple myeloma patients : a case control study. 27(11):1–4, 2008.

[26] Ken-Ichi Tezuka, Yoshitaka Wada, Akiyuki Takahashi, and Masanori Kikuchi. Computer-simulated bone architecture in a simple bone-remodeling model based on a reaction-diffusion system. *J Bone Miner Metab*, 23(1):1–7, January 2005.

[27] Eberhard O. Voit. *Computational analysis of biochemical systems: a practical guide for biochemists and molecular biologists*. Cambridge University Press, Cambridge; New York, 2000.

[28] Ronald Walker, Bart Barlogie, Jeffrey Haessler, Guido Tricot, Elias Anaissie, John D. Shaughnessy, Joshua Epstein, Rudy van Hemert, Eren Erdem, Antje Hoering, John Crowley, Ernest Ferris, Klaus Hollmig, Frits van Rhee, Maurizio Zangari, Mauricio Pineda-Roman, Abid Mohiuddin, Shmuel Yaccoby, Jeffrey Sawyer, and Edgardo J. Angtuaco. Magnetic Resonance Imaging in Multiple Myeloma: Diagnostic and Clinical Implications. *J Clin Oncol*, 25(9):1121–8, March 2007.

[29] Yan Wang, Peter Pivonka, Pascal R Buenzli, David W Smith, and Colin R Dunstan. Computational Modeling of Interactions between Multiple Myeloma and the Bone Microenvironment. *PloS one*, 6(11):e27494, January 2011.

[30] Jinhu Xiong, Melda Onal, Robert L Jilka, Robert S Weinstein, Stavros C Manolagas, and Charles a O'Brien. Matrix-embedded cells control osteoclast formation. *Nature medicine*, 17(10):1235–41, October 2011.